ISSN 1070-3632, Russian Journal of General Chemistry, 2018, Vol. 88, No. 6, pp. 1103–1107. © Pleiades Publishing, Ltd., 2018.
Original Russian Text © A.D. Antuf'eva, D.R. Akhmatzyanova, M.V. Dmitriev, E.V. Shklyaeva, G.G. Abashev, 2018, published in Zhurnal Obshchei Khimii, 2018, Vol. 88, No. 6, pp. 922–926.

Synthesis and Structure of 2-(1*H*-Indol-1-yl)-6-ferrocenyl-4-(2-chloroimidazo[1,2-*a*]pyridin-3-yl)pyrimidine

A. D. Antuf'eva[a], D. R. Akhmatzyanova[b], M. V. Dmitriev[b], E. V. Shklyaeva[b,c], and G. G. Abashev[a–c]*

[a] *Institute of Technical Chemistry, Perm Federal Research Center, Ural Branch, Russian Academy of Sciences, ul. Akademika Koroleva 3, Perm, 614013 Russia*
**e-mail: gabashev@psu.ru*

[b] *Perm State National Research University, Perm, Russia*

[c] *Institute of Natural Sciences, Perm State National Research University, Perm, Russia*

Received January 15, 2018

Abstract—A 2,4,6-trisubstituted pyrimidine including a 2-(1*H*-indol-1-yl) substituent was synthesized by the reaction of 1-ferrocenyl-3-(2-chloroimidazo[1,2-*a*]pyridin-3-yl)propanone with 2,5-dimethoxytetrahydrofuran. The structure of the synthesized compound was confirmed by IR and ^{1}H NMR spectroscopy, and X-ray diffraction analysis. It has been shown that the ferrocene-containing compounds synthesized in the present work all demonstrate intramolecular charge transfer which is evidenced by the observation of the corresponding absorption bands with $\lambda_{max}^{abs} > 480$ nm. The oxidation potential of ferrocene (E_{ox}^{Fc}) in all the compounds is higher than 700 mV.

Keywords: indole, 2-aminopyrimidine, ferrocene, 1-azaindolizine, 2,5-dimethoxytetrahydrofuran, Clauson–Kaas reaction

DOI: 10.1134/S1070363218060099

Heterocyclic structures incorporating both the pyrimidine and indole fragments have fairly long been known. Substituted fused 9*H*-pyrimido[4,5-*b*]indoles first described by Glushkov et al. [1] are an important class of such compounds [2, 3]. Pyrimidines, where the indole fragment is linked to the pyrimidine nucleus via the C^3 atom of the indole ring, have also been reported; such structures are most commonly synthesized by the condensation of chalcones with urea or thiourea [4]. Pyrimidines linked to the indole fragment via the nitrogen atom of the latter, specifically substituted 1-(pyrimidin-2-yl)-1*H*-indoles, are less known; such structures most frequently contain a substituted indole fragment. They can be synthesized either by the reactions of substituted or unsubstituted indoles with 2-chloropyrimidine under the action of sodium hydride in DMF or alkali metal carbonates in DMSO [5] or PEG 400 by ultrasonication [6] or by Ru-catalyzed reactions of substituted *N*-(pyrimidin-2-yl)anilines with diarylacetylenes [7]. Aimed at preparing new ferrocene-containing chromophores, we have developed a different synthetic approach to such compounds. The key stage of this process is the Clauson–Kaas reaction. As a result, we obtained a previously unknown Y-shaped chromophore of DAD' motif, where A is the central electron-deficient core consisting of the pyrimidine and 2-chloroimidazo[1,2-*a*]-pyridine and D and D' are the electron excessive feroccene and indole substituents in the 6- and 2-positions of the pyrimidine ring. The reaction sequence used in the present work is shown in the Scheme 1.

To form the future 1-azaindolizine fragment, we treated 2-aminopyridine by chloroacetic acid to obtain 2-(2-imino-1,2-dihydropyridin-1-yl)acetic acid **1** [8], and the latter was cyclized under the action of $POCl_3$ to obtain 2-chloroimidazo[1,2-*a*]pyridine **2** [8] and then aldehyde **3**, whose structure was confirmed by X-ray diffraction analysis [9]. The condensation of adehyde **3** with acetylferrocene gave rise to chalcone **4** [9], which

Scheme 1.

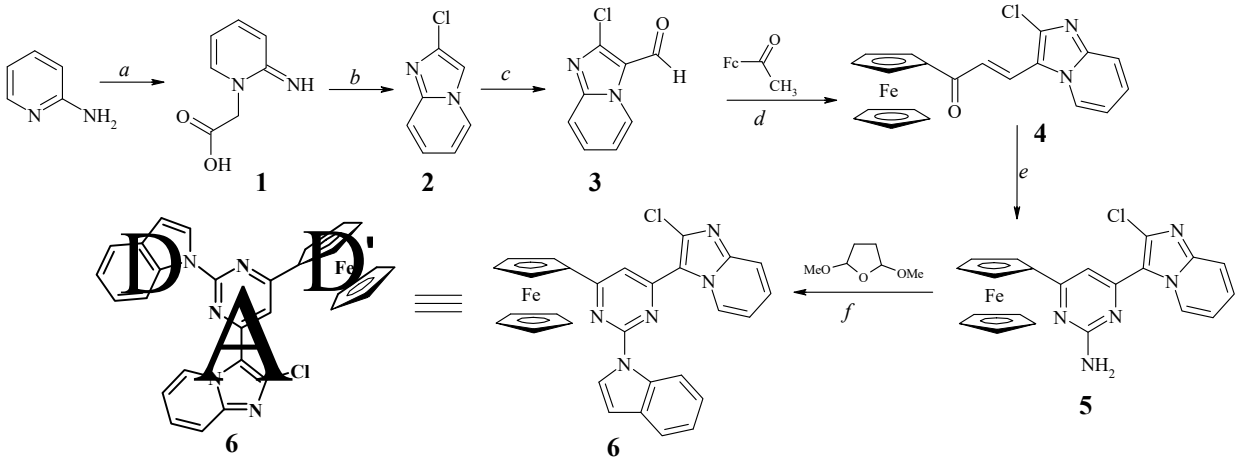

Reaction conditions: *a*, $ClCH_2COOH$, Et_3N, H_2O, 90°C, 5 h; *b*, $POCl_3$, toluene, 110°C, 16 h; *c*, $POCl_3$, DMF, PhCl, 70°C, 5 h; *d*, 2% NaOH (aq.), reflux for 5 h; *e*, guanidine sulfate, 50% KOH–EtOH, reflux for 3 h, then H_2O_2, (33%), reflux for1 h; *f*, AcOH, reflux, 4 h.

was then used to prepare 4,6-disubstituted 2-aminopyrimidine **5**. The target product **6** was synthesized by the Clauson–Kaas reaction (a modified version of the Paal–Knorr reaction). Depending on the reaction conditions, the amino group in the 2-position of the pyrimidine ring can be converted into the pyrrole [10–15], indole [15], or carbazole rings [16, 17]. The potentialities of this reaction was briefly presented by Husson et al. [18] in their review on the synthetic applications of 2,5-dimethoxytetrahydrofuran. Pyrimidine **6** is a bright red crystalline substance. Its composition and structure were confirmed by elemental analysis, IR and ^{1}H NMR spectroscopy, and X-ray diffraction analysis (Fig. 1).

Pyrimidine **6** crystallizes in a monoclinic centrosymmetric space group. The ferrocene fragment has a geometry typical for such structures, with the two cyclopentadienyl fragments in an eclipsed conformation. The pyrimidine ring is planar within 0.01 Å, and it is almost coplanar with the cyclopentadienyl ring: the dihedral angle between the pyrimidine and $C^{20}C^{21}C^{22}C^{23}C^{24}$ ring planes is 3.9°. The imidazopyridine and indole fragments are planar within 0.04 and 0.03 Å, and the dihedral angles between these ring planes and the pyrimidine ring lane are 17.9° and 8.7°, respectively. The main feature of the crystal structure is that the molecules are packed in stacks, where the aromatic fragments of adjacent molecules are so close to each that the resulted distance between them: the centroid-to-centroid distances between the benzo and imidazole rings and the pyrimidine and pyrrole rings span the range 3.5–3.7 Å (Fig. 2).

The UV spectra of pyrimidine **6** were studied in comparison with those of the starting compounds: chalcone **4** and 2-aminopyrimidine **5**. Figure 3 compares the UV spectra of chloroform solution of compounds **4**–**6** (the absorption intensities are normalized). The values of the absorption maxima, absorption edge and optical band gaps are summarized in the table. As seen from these data, compounds **4**–**6** absorb in the visible region; the widest absorption range is inherent to chalcone **4** (λ_{onset}^{abs} 600 nm); besides, this very compound has also the most intense and long wavelength absorption maximum (λ_{max}^{abs} 510 nm) arising from the efficient intramolecular charge transfer (ICT). Furthermore, chalcone **4** has the narrowest optical band gap (E_g^{opt} ~2 eV).

We have also studied the electrochemical behavior of pyrimidine **6** and its parent compounds **4** and **5** by means of cyclic voltammetry (see table). Figure 4 presents the comparison of voltammograms (CVs) of pyrimidines **5** and **6** cyclic. All of the obtained CVs show one reversible oxidation peak associated with the redox process in the ferrocene fragment. The highest Fc/Fc^+ redox potential has been observed for chalcone **4** (740 mV), which is explained by the presence of an electron-deficient propenone fragment. The CVA of pyrimidine **6**, which contains the indole fragment, displays the second, weak irreversible one-electron absorption

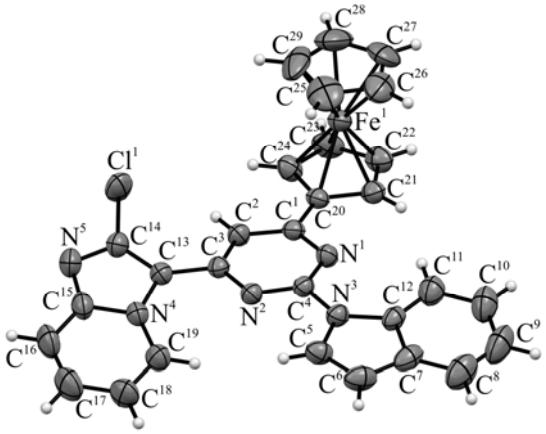

Fig. 1. General view of a molecule of compound **6** in crystal.

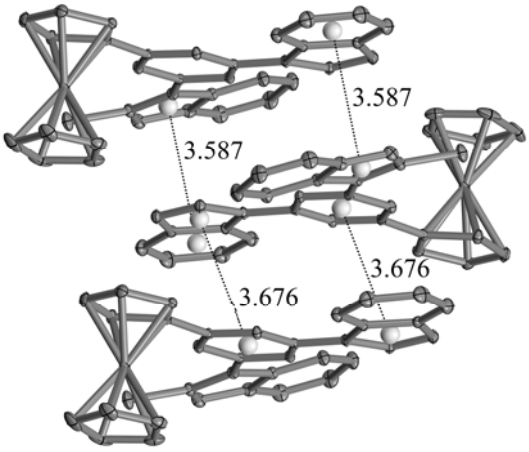

Fig. 2. Crystal packing of molecules of compound **6**.

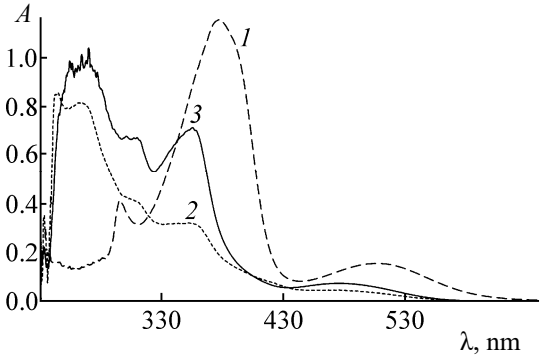

Fig. 3. Comparison of the (*1–3*) UV spectra of compounds **4**–**6** in $CHCl_3$ ($c = 1\times10^{-3}$ M).

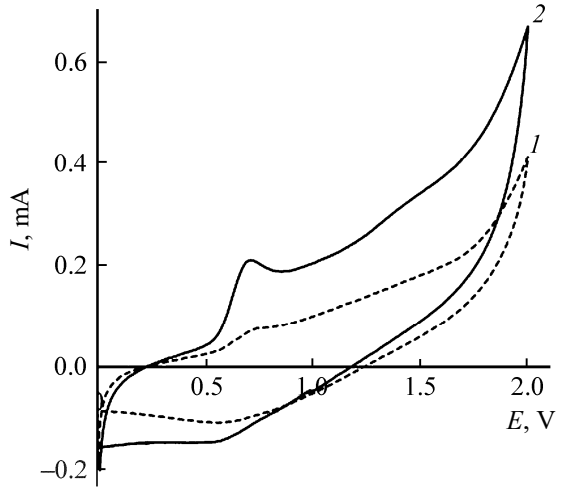

Fig. 4. Comparison of the CVAs of compounds (*1*) **5** and (*2*) **6** ($c = 0.1$ M, MeCN–CH_2Cl_2, Et_4ClO_4).

wave (E^1_{ox} ~1.38 V), associated with the dimer formation due to the oxidation of the indole fragment.

EXPERIMENTAL

The IR spectra were measured on a Perkin–Elmer Spectrum Two FTIR spectrometer for suspensions in mineral oil. The NMR spectra were obtained on a Varian Mercury Plus300 spectrometer (300 MHz) in $CDCl_3$, internal reference HMDS. The melting/decomposition points were measured by a Mettler Toledo MP70 instrument. The reaction progress was monitored and the purity of the synthesized compounds were controlled by TLC (Sorbfil, Silufol). The mixtures of compounds and the target products were purified in silica columns (Alfa-Aesar, Silica gel 60, 0.060–0.2 mm). The UV spectra were run on a Shimadzu UV-2600 spectrophotometer, cell length 10 mm, solvent $CHCl_3$ ($c = 1\times10^{-5}$ M). Electrochemical measurements were performed on a Gamry Interface1000 potentiostat in a three-electrode cell with a carbositall working electrode, a platinum auxiliary electrode, and a silver–silver chloride reference electrode. In the experiments we used millimolar solutions of the samples in a mixture of anhydrous MeCN and CH_2Cl_2 (4 : 1, 10 mL), background electrolyte Et_4NClO_4 ($c = 0.1$ M), potential scan rate (v_{scan}) 50 mW/s. Elemental analysis (C, H) was performed on a Vario EL Cube analyzer. The iron content was estimated using a Thermo iCE 3500 adsorption sectrometer.

Acetylferrocene was purified from diacetylferrocene by the procedure in [20].

3-(2-Chloroimidazo[1,2-*a*]pyridin-3-yl)-1-ferrocenylpropenone (4). A suspension of 2.3 g (0.01 mol)

Optical and electrochemical characteristics of compounds **4**–**6**

Comp. no.	λ_{max}^{abs}, nm	λ_{onset}^{abs}, nm	E_g^{opt}, eV[a]	E_{ox}^{Fc}, mV	E_{red}^{Fc}, mV	E_{ox}^{1}, mV
4	295, 377, 510	607	2.04	740	630	
5	244, 266, 312, 389, 489	529	2.34	720	610	
6	262, 306, 355, 481	541	2.29	710	580	1380

[a] $E_g^{opt} = 1240\ \lambda_{onset}^{abs}$ [19].

of acetylferrocene and 1.8 g (0.01 mol) of 2-chloroimidazo[1,2-*a*]pyridine-3-carbaldehyde **3** in 100 mL of 2% NaOH was heated for 2 h, cooled, and poured into water with ice. The precipitate was filtered off and purified by column chromatography (eluent hexane–acetone, 3 : 1). Yield 85%, mp 178–180°C (mp 180°C [9]), red crystals.

2-Amino-4-(2-chloroimidazo[1,2-*a*] pyridin-3-yl)-6-ferrocenylpyrimidine (5) was prepared by the procedure in [21]. A mixture of 2.5 g (6.5 mmol) of 3-(2-chloroimidazo[1,2-*a*]pyridin-3-yl)-1-ferrocenylpropenone **4** and 1.57 g (10 mmol) of guanidine sulfate in 50 mL of ethanol was stirred for 15–20 min with 5 mL of 50% aqueous KOH and refluxed for 3 h. Water, 3 mL, was then added in small portions under the same conditions and refluxing was continued for an additional 1 h. The hot reaction mixture was poured into water with ice, the precipitate was filtered off, dried in air, and purified by column chromatography (eluent hexane–acetone, 1 : 1). Yield 45%, mp 87–89°C, dark red crystals. IR spectrum, ν, cm^{-1}: 3275, 3421 (NH_2). ^{1}H NMR spectrum ($CDCl_3$), δ, ppm (*J*, Hz): 4.21 s (5H, Fc), 4.55 t (2H, Fc, ^3J = 1.8), 4.89 t (2H, Fc, ^3J = 1.8), 5.05 br s (2H, NH_2), 6.98 s (1H, pyrimidine), 7.47 d (2H, C_6H_4, ^3J = 8.7), 7.61 d (2H, C_6H_4, ^3J = 9.0). Found, %: C 59.05; H 3.64; Fe 12.94. $C_{21}H_{16}ClFeN_5$. Calculated, %: C 58.70; H 3.75; Fe 13.00.

2-Indolyl-4-(2-chloroimidazo[1,2-*a*]pyridin-3-yl)-6-ferrocenylpyrimidine (6). A solution of 0.7 g (2 mmol) of 2-aminopyrimidine in 5 mL of glacial acetic acid containing 0.5 mL (3.0 mmol) of 2,5-dimethoxytetrahydrofuran was heated under reflux for 4 h, heated, and poured into 150 mL of water with ice. The precipitate was filtered off and purified by column chromatography. Yield 48%, mp 104–106°C, dark red crystals. ^{1}H NMR spectrum ($CDCl_3$), δ, ppm (*J*, Hz): 4.19 s (5H, Fc), 4.62 m (2H, Fc), 5.19 m (2H, Fc), 6.76 d (1H, indole pyrrole, ^3J = 3.6), 7.05 m (1H, imidazole), 7.29 t (1H, indole, ^3J = 7.5), 7.38 t (1H, indole, ^3J = 7.5), 7.44 m (1H, imidazole), 7.67 d (1H, indole, ^3J = 7.8), 7.83–7.87 m (1H, indole), 8.31 d (1H, indole pyrrole, ^3J = 3.6), 8.87 d (1H, indole, ^3J = 8.1), 9.7 m (1H, pyrimidine)

X-ray diffraction analysis of compound 6 was performed on an Xcalibur Ruby diffractometer with a CCD detector by a standard procedure (ω scanning with a 1° step) at 295(2) K with a MoK_α radiation (λ 0.71073 Å) and a graphite monochromator [22]. A dark red needle-like crystal 0.55×0.09×0.03 mm in dimensions was used. Monoclinic syngony, space group $P2_1/c$, *a* 12.318(2), *b* 7.3115(14), *c* 25.793(4) Å, β 97.262(17)°, *V* 2304.4(8) $Å^3$, $C_{29}H_{20}ClFeN_5$, *Z* 4. Final refinement parameters: R_1 0.0505, wR_2 0.1140 [for 3800 reflections with $I > 2\sigma(I)$], R_1 0.0805, wR_2 0.1337 (for all 5435 unique reflections), *S* 1.031. Maximal and minimal residual electron density peaks: 0.364 and –0.335 $\bar{e}/Å^3$. Absorption was included empirically using SCALE3 ABSPACK algorithm [22]. The structure was decoded by a direct method and refined by full-matrix least squares on F^2 in the anisotropic approximation for nonhydrogen atoms. The hydrogen atoms were placed in geometric positions and refined riding on their carrier atoms isotropically with dependent thermal parameters. ShELXS-97 [23, 24] and OLEX2 program suits [25] were used for structure solution and refinement. The resulting crystallographic information was deposited in the Cambridge Crystallographic Data. Center (CCDC 1845553).

ACKNOWLEDGMENTS

Instrumental investigations were performed using the equipment acquired at the expense of the Program for the development of National Research Universities.

REFERENCES

1. Glushkov, R.G., Volskova, V.A., and Magidson, O.Y., *Pharm. J. Chem*., 1967, vol. 1, p. 517. doi 10.1007/BF00770336
2. Golubev, A.S., Mityushina, O.A., Shidlovskii, A.F., Suponitsky, K.Yu., and Chkanikov, N.D., *Fluorine*

Notes, 2014, vol. 87, no. 6. http://ru.notes.fluorine1.ru/public/2014/6_2014/letters/index.html.

3. Lauria, A., Diana, L.P., Barraja, P., Montalbano, A., Dattolo, G., Cirrincione, G., and Almerico, A.M., *Arkivoc*, 2004, no. 5, p. 263.
4. Nassar, E., El-Badry, Y.A., Eltoukhy, A.M.M. and Ayyad, R.R., *Med. Chem*., 2016, vol. 6, p. 224. doi 10.4172/2161-0444.1000350
5. Ackermann, L. and Lygin, A.V., *Org. Lett*., 2011, vol. 13, p. 3332. doi 10.1021/ol2010648.
6. Sailaja, E., Bhavani, S., Rambabu, D., Rao Basaveswara, M.V., and Pal, M., *Arab. J. Chem*., 2015. doi 10.1016/j.arabjc.2015.11.008
7. Ackermann, L. and Lygin, A.V., *Org. Lett*., 2012, vol. 14, p. 764. doi 10.1021/ol203309y
8. Maxwel, B.D., Boye, O.G., and Ohta, K., *J. Label. Compd. Radiopharm*., 2005, vol. 48, p. 397. doi 10.1002/jlcr.934
9. Akhmatzyanova, D.R., Antuf'eva, A.D., Shklyaeva, E.V., and Abashev, G.G., *Vestn. Perm. Univ. Khim*., 2016, vol. 24, no. 4, p. 61.
10. Shklyaeva, E.V., Bushueva, A.Yu., Romanova, V.A., and Abashev, G.G., *Russ. J. Org. Chem*., 2010, vol. 46, p. 938. doi 10.1134/S1070428010060308
11. Bushueva, A.Yu., Abashev, G.G., and Shklyaeva, E.V., *Mendeleev Commun*., 2009, vol. 19, p. 329.
12. Antuf'eva, A.D., Zhulanov, V.E., Dmitriev, M.B., Mokrushin, I.G., Shklyaeva, E.V., and Abashev, G.G., *Russ. J. Gen. Chem*., 2017, vol. 87, p. 470. doi 10.1134/S1070363217030161
13. Kiskan, B., Gacal, B., Asan, M., Comert Gunaydin, E., Yilmaz, I., and Yagci, Y., *Polym. Bull*., 2011, vol. 67, p. 609. doi 10.1007/s00289-010-0412-9
14. Josey, A.D. and Jenner, E.L., *J. Org. Chem*., 1962, vol. 27, p. 2466. doi 10.1021/jo01054a042
15. Lee, D.H., Lee, S.G., Lung, D.J., and Hahn, J.T., *Asian J. Chem*., 2013, vol. 25, p. 501. doi 10.14233/ajchem.2013.13307
16. Kashima, C., Hibi, S., Maruyama, T., and Omote, Y., *Tetrahedron Lett*., 1986, vol. 27, p. 2131. doi 10.1016/S0040-4039(00)84467-6
17. Kashima, C., Hibi, S., and Maruyama, T., *J. Heterocycl. Chem*., 1987, vol. 24, p. 913. doi 10.1002/jhet.5570240405
18. Husson, H.-P., Royer, J., Rochais, C., and Dallemagne, P., *e-EROS Encyclopedia of Reagents for Organic Synthesis*, 2012. doi 10.1002/047084289X.rd289.pub2
19. Meng, H., Zheng, J., Lovinger, A.J., Wang, B.-C., Van Patten, P.G., and Bao, Z., *Chem. Mater*., 2003, vol. 15, p. 1778. doi 10.1021/cm020866z
20. Wang, R., Hong, X., and Shan, Z., *Tetrahedron Lett*., 2008, vol. 49, p. 636. doi 10.1016/j.tetlet.2007.11.119
21. Varga, L., Nagy, T., Kovesdi, I., Benet-Buchholz, J., Dorman, G., Urge, L., and Darvas, F., *Tetrahedron*, 1959, vol. 59, p. 655. doi 10.1016/S0040-4020(02)01560-0
22. *CrysAlisPro*, Agilent Technologies, Version 1.171.37.33 (release 27-03-2014 CrysAlis171.NET).
23. Sheldrick, G.M., *Acta Crystallogr., Sect. A*, 2008, vol. 64, p. 112. doi 10.1107/S0108767307043930
24. Sheldrick, G.M., *Acta Crystallogr., Sect. C*, 2015, vol. 71, p. 3. doi 10.1107/S2053229614024218
25. Dolomanov, O.V., Bourhis, L.J., Gildea, R.J., Howard, J.A.K., and Puschmann, H., *J. Appl. Crystallogr*., 2009, vol. 42, p. 339. doi 10.1107/S0021889808042726